

Research Article

Dissociation of J/ψ and Y Using Dissociation Energy Criteria in N -Dimensional Space

Siddhartha Solanki , Manohar Lal , and Vineet Kumar Agotiya 

Department of Physics, Central University of Jharkhand, 835222, Ranchi, India

Correspondence should be addressed to Vineet Kumar Agotiya; agotiya81@gmail.com

Received 25 November 2023; Revised 13 March 2024; Accepted 26 March 2024; Published 8 April 2024

Academic Editor: Bhartendu K. Singh

Copyright © 2024 Siddhartha Solanki et al. This is an open access article distributed under the Creative Commons Attribution License, which permits unrestricted use, distribution, and reproduction in any medium, provided the original work is properly cited. The publication of this article was funded by SCOAP³.

The analytical exact iteration method (AEIM) has been widely used to calculate N -dimensional radial Schrodinger equation with medium-modified form of Cornell potential and is generalized to the finite value of magnetic field (eB) with quasiparticle approach in hot quantum chromodynamics (QCD) medium. In N -dimensional space, the energy eigenvalues have been calculated for any states (n, l). These results have been used to study the properties of quarkonium states (i.e. the binding energy and mass spectra, dissociation temperature, and thermodynamical properties in the N -dimensional space). We have determined the binding energy of the ground states of quarkonium with magnetic field and dimensionality number. We have also determined the effects of magnetic field and dimensionality number on mass spectra for ground states of quarkonia. But the main result is quite noticeable for the values of dissociation temperature in terms of magnetic field and dimensionality number for ground states of quarkonia after using the criteria of dissociation energy. At last, we have also calculated the thermodynamical properties of QGP (i.e., pressure, energy density, and speed of sound) using the parameter eB with ideal equation of states (EoS). A preprint has previously been published (Solanki et al., 2023).

1. Introduction

The system of heavy quarkonia (such as bottomonium and charmonium) has played a key role for the comprehensive and quantitative test of quantum chromodynamics (QCD) and the standard model [1]. After the discovery of J/ψ in 1974, the study of heavy quarkonia becomes an interesting topic for both the theoretical and experimental high energy physics. The radial Schrodinger equation has been solved with the real part of medium-modified form of Cornell potential [2]. The Cornell potential, or Cornell potential model, is used in the context of heavy quarkonia, specifically to describe the interaction between a quark and an antiquark within these mesonic systems. Here, we refer to several phenomena like the quark confinement, mathematical analysis and interpretation of the bound state, spectroscopy and properties of heavy quarkonia, phenomenological modeling of QCD with aim to bridge the gap between theoretical predictions and experimental observations, prediction of various properties of quarkonia such as energy levels and

decay rates, and other spectroscopic features, and the solution, thus, obtained can be used to understand many phenomena in the study of atomic and molecular physics, spectroscopy (hadronic as well as molecular), nuclear physics, and also high energy physics which are not yet understood. Most of the recent quarkonium studies are focused on N -dimensional space problem [3] and lower spatial or dimensional space problem [4]. The consequences of N -dimensional space have been considered for energy levels of the bound state system of quarkonia [5]. In the N -dimensional space, the study of the harmonic oscillator [6] and hydrogen atom [7] has also been done. Additionally, in N -dimensional space, the Schrodinger equation has also been solved for potentials such as Cornell potential [8], fourth-order inverse power potential [9], Mie-type potential [10], Kratzer potential [11], Coulomb potential [12], energy-dependent potential [13, 14], global potential [15], Hua potential [13, 14], and harmonic potential [3].

There were several methods used to solve the Schrodinger equation such as power series method [1], Hill-determinant method [16], numerical methods [17–19], quasilinearization

method (QLM) [20], point canonical transformation (PCT) [21], operator algebraic method [22], Nikiforov-Uvarov (UV) method [5, 13, 14, 23], power series technique [24], Laplace transformation methods [3, 12], asymptotic iteration method (AIM) [2], SUSYQM method, AEIM [25], and Pekeris-type approximation [13, 14, 26].

The quarkonium dissociation rates for the ground state have been studied by direct continuum of thermal activation, tunneling, binding energy, and phase shift scattering in the hot quark-gluon plasma (QGP) for the eigenstates of the lowest values [18, 27]. Vija and Thoma [28] extended perturbed gauge theory for the collisional energy loss in QGP at finite chemical potential and temperature. The quarkonium dissociation has been studied by correcting Cornell potential via hard thermal loop-resummed propagator of the gluon [29, 30]. The study of the heavy quarkonium binding energy in details is found in [31, 32], and the chemical potential effect has been also studied by the methods of dissipative hydrodynamic on quark-gluon plasma, production of photon in QGP, and quark-gluon plasma thermodynamical properties [33–37]. Alberico et al. [38], Mocsy and Petreczky [39], and Agotiya et al. [40] have solved the Schrodinger equation for the quarkonium states at finite temperature, using a temperature-dependent effective potential by the linear combination of internal energy, and concluded the spectral function of quarkonium in a quark-gluon plasma.

From previously published articles, we study about the effect of baryonic chemical potential incorporated by the quasiparticle Debye mass [41] for finding the properties of quarkonium. In this work, we follow the recently published preprint work [42] to investigate quarkonium dissociation using dissociation energy criteria with the effect of magnetic field that has been introduced through quasiparticle Debye mass. We have used the medium-modified form of potential, so formed, obtaining the binding energies and mass spectra in N -dimensional space of charmonium and bottomonium at different values of magnetic field and dimensionality number. The dissociation energy of QGP has been introduced for the calculation of dissociation temperature of the ground states of quarkonia by the intersection point of dissociation energy and binding energy in N -dimensional space. In other studies, authors have also calculated the dissociation temperature by using the criteria that at dissociation point thermal width is equal to twice of binding energy. The effect of magnetic field and dimensionality number significantly revise values of dissociation points. At last, we have also calculated the thermodynamical properties of QGP (i.e., pressure, energy density, and speed of sound) using the eB and dimensionality number (N) and compared with the previous published data.

The paper is organized as follows: in Section 2, the exact solution of N -dimensional radial Schrodinger equation with the medium-modified form of Cornell potential has been calculated. In Section 3, quasiparticle model and Debye mass have been discussed. In Section 4, the binding energy of quarkonium state in N -dimensional space has been investigated. In Section 5, a brief description about the mass spectra of quarkonium state in N -dimensional space has been provided. In Section 6, the study about the QCD EoS in

the presence of eB has been discussed. In Section 7, the dissociation energy (D.E.) of quarkonium state in N -dimensional space has been investigated. Results have been discussed in Section 8, and this work has been concluded in Section 9.

2. The Solution of N -Dimensional Radial Schrodinger Equation with the Medium-Modified Form of Cornell Potential

The N -dimensional radial Schrodinger equation for two interacting particles has been solved for the medium-modified form of the Cornell potential using AEIM [43, 44].

$$\frac{d^2}{dr^2} + \frac{N-1}{r} \frac{d}{dr} - \frac{l(l+N-2)}{r^2} + 2\mu_{Q\bar{Q}}[E_{nl} - V(r)]\psi(r) = 0, \quad (1)$$

where N , l , and $\mu_{Q\bar{Q}}$ are the dimensional number, angular quantum number, and reduced mass of bound state, respectively. Now, the wave function $[\psi(r)]$ chosen here is

$$\psi(r) = \frac{R(r)}{r^{(N-1)/2}}. \quad (2)$$

Putting Eq. (2) in Eq. (1), we get

$$\left[\frac{d^2}{dr^2} - \frac{\lambda^2 - (1/4)}{r^2} + 2\mu_{Q\bar{Q}}[E_{nl} - V(r)] \right] R(r) = 0. \quad (3)$$

where

$$\lambda = l + \left(\frac{N-2}{2} \right). \quad (4)$$

We have taken the spatially isotropic form of heavy quark Cornell potential to obtain the in-medium modification, i.e.,

$$V(r) = -\frac{\alpha}{r} + \sigma r. \quad (5)$$

In general, the spatial form of the potential may have anisotropic structure due to the breaking of spherical symmetry in the presence of magnetic field [45, 46]. In our work, the in-medium modification of the above equation (Eq. (5)) has been obtained in the momentum space by dividing the vacuum heavy quark potential with the medium dielectric permittivity [46], which carries the information of temperature and magnetic field (eB). In that case, we have found that the in-medium-modified form of Cornell potential [47] for the study of quarkonia in the presence of eB is as follows:

$$V(r) = \frac{\sigma}{m_D} [1 - \exp(-m_D r)] - \frac{\alpha}{r} [\exp(-m_D r)]. \quad (6)$$

Using exponential formula $e^{-m_D r} = \sum_{k=0}^{\infty} ((-m_D r)^k / k!)$ for solving Eq. (5) and neglecting the higher orders at $m_D r \ll 1$, thus Eq. (6) takes the following form:

$$V(r) = -ar^2 + br + c - \frac{d}{r}, \quad (7)$$

where the values of a , b , c , and d are given as $a = (1/2)(\sigma m_D)$, $b = (1/2)(2\sigma - \alpha m_D^2)$, $c = \alpha m_D$, and $d = \alpha$; substituting these values in Eq. (3), we get the radial wave function:

$$R''(r) = \left[-\varepsilon_{nl} - a_1 r^2 + b_1 r + c_1 - \frac{d_1}{r} + \frac{\lambda^2 - (1/4)}{r^2} \right] R(r), \quad (8)$$

where $\varepsilon_{nl} = 2\mu_{Q\bar{Q}} E_{nl}$, $a_1 = |-2\mu_{Q\bar{Q}} a|$, $b_1 = 2\mu_{Q\bar{Q}} b$, $c_1 = 2\mu_{Q\bar{Q}} c$, and $d_1 = 2\mu_{Q\bar{Q}} d$. AEIM requires making the following ansatz for the wave function as in [11, 48, 49].

$$R(r) = f_n(r) \exp [g_1(r)], \quad (9)$$

where

$$f_n(r) = 1, \quad (10)$$

if $n = 0$, and

$$f_n(r) = \prod_{i=1}^n (r - \alpha_i^{(n)}), \quad (11)$$

if $n = 1, 2, 3, \dots$.

$$g_1(r) = -\frac{1}{2} \alpha r^2 - \beta r + \delta \ln r, \quad \alpha > 0, \beta > 0. \quad (12)$$

From Eq. (8), we get

$$R''_{n,l}(r) = \left(g''_l(r) + g'_l{}^2(r) + \frac{f''_n(r) + 2g'_l(r)f'_n(r)}{f_n(r)} \right) R_{n,l}(r). \quad (13)$$

After comparing Eq. (13) and Eq. (9), we have

$$\begin{aligned} -\varepsilon_{n,l} + a_1 r^2 + b_1 r + c_1 - \frac{d_1}{r} + \frac{\lambda^2 - (1/4)}{r^2} \\ = g''_l(r) + g'_l{}^2(r) + \frac{f''_n(r) + 2g'_l(r)f'_n(r)}{f_n(r)}. \end{aligned} \quad (14)$$

At $n = 0$, substituting Eqs. (10)–(13) into Eq. (14), we get

$$\begin{aligned} a_1 r^2 + b_1 r + c_1 - \frac{d_1}{r} + \frac{\lambda^2 - (1/4)}{r^2} - \varepsilon_{0l} \\ = \alpha^2 r^2 + 2\alpha\beta r - \alpha[1 + 2(\delta + 0)] \\ + \beta^2 - \frac{2\beta\delta}{r} + \frac{\delta(\delta - 1)}{r^2}. \end{aligned} \quad (15)$$

Now, comparing the coefficient of r on both side of Eq. (15), we obtain

$$\begin{aligned} \alpha &= \sqrt{a_1}, \\ \beta &= \frac{b_1}{2\sqrt{a_1}}, \\ d_1 &= 2\beta(\delta + 0), \\ \delta &= \frac{1}{2}(1 \pm 2\lambda), \\ \varepsilon_{0l} &= \alpha[1 + 2(\delta + 0)] + C_1 - \beta^2. \end{aligned} \quad (16)$$

Now, the energy eigenvalue for the ground state is as follows:

$$E_{0l} = \sqrt{\frac{a}{2\mu_{Q\bar{Q}}}}(N + 2l) + C - \frac{b^2}{4(\sqrt{a})^2}. \quad (17)$$

Now, for the first node ($n = 1$), we used the functions $f_1(r) = (r - \alpha_1^{(1)})$ and $g_1(r)$; then,

$$\begin{aligned} a_1 r^2 + b_1 r + c_1 - \frac{d_1}{r} + \frac{\lambda^2 - (1/4)}{r^2} - \varepsilon_{1l} \\ = \alpha^2 r^2 + 2\alpha\beta r - \alpha[1 + 2(\delta + 1)] + \beta^2 \\ - \frac{2[\beta(\delta + 1) + \alpha\alpha_1^{(1)}]}{r} + \frac{\delta(\delta - 1)}{r^2}. \end{aligned} \quad (18)$$

By comparing the coefficients of r , the relation between the potential parameters is as follows:

$$\begin{aligned} \alpha &= \sqrt{a_1}, \\ \beta &= \frac{b_1}{2\sqrt{a_1}}, \\ d_1 &= 2\beta(\delta + 1), \\ \delta &= \frac{1}{2}(1 \pm 2\lambda), \\ \varepsilon_{1l} &= \alpha[1 + 2(\delta + 1)] + C_1 - \beta^2, \\ d_1 - 2\beta(\delta + 1) &= 2\alpha\alpha_1^{(1)}, \\ (d_1 - 2\beta\delta)\alpha_1^{(1)} &= 2\delta. \end{aligned} \quad (19)$$

Now, the energy eigenvalue formula for first excited state E_{1l} is as follows:

$$E_{1l} = \sqrt{\frac{a}{2\mu_{Q\bar{Q}}}}(N + 2l + 2) + C - \frac{b^2}{4(\sqrt{a})^2}. \quad (20)$$

Similarly, for the second node ($n = 2$), we use $f_2(r) = (r - \alpha_1^{(2)})(r - \alpha_2^{(2)})$ and $g_1(r)$ and we get

$$\begin{aligned}
& a_1 r^2 + b_1 r + C_1 - \frac{d_1}{r} + \frac{\lambda^2 - (1/4)}{r^2} - \varepsilon_{2l} \\
& = \alpha^2 r^2 + 2\alpha\beta r - \alpha[1 + 2(\delta + 2)] + \beta^2 \\
& - \frac{2[\beta(\delta + 2) + \alpha(\alpha_1^{(2)} + \alpha_2^{(2)})]}{r} + \frac{\delta(\delta - 1)}{r^2}.
\end{aligned} \quad (21)$$

By comparing the coefficients of r , we get

$$\begin{aligned}
\alpha &= \sqrt{a_1}, \\
\beta &= \frac{b_1}{2\sqrt{a_1}}, \\
\delta &= \frac{1}{2}(1 \pm 2\lambda), \\
\varepsilon_{2l} &= \alpha[1 + 2(\delta + 2)] + C_1 - \beta^2,
\end{aligned}$$

$$d_1 - 2\beta(\delta + 2) = 2\alpha(\alpha_1^{(2)} + \alpha_2^{(2)}),$$

$$(d_1 - 2\beta\delta)\alpha_1^{(2)}\alpha_2^{(2)} = 2\delta(\alpha_1^{(2)} + \alpha_2^{(2)}),$$

$$d_1 - 2\beta(\delta + 1)(\alpha_1^{(2)} + \alpha_2^{(2)}) = 4\alpha(\alpha_1^{(2)}\alpha_2^{(2)}) + 2(2\delta + 1). \quad (22)$$

The energy eigenvalue for E_{2l} is as follows:

$$E_{2l} = \sqrt{\frac{a}{2\mu_{Q\bar{Q}}}}(N + 2l + 4) + C - \frac{b^2}{4(\sqrt{a})^2}. \quad (23)$$

Hence, with the repetition of the iteration method, the approximate energy eigenvalue for the quarkonium states depending upon the temperature and magnetic field in the N -dimensional space becomes

$$E_{nl}^n = \sqrt{\frac{a}{2\mu_{Q\bar{Q}}}}(N + 2l + 2n) + C - \frac{b^2}{4(\sqrt{a})^2}, \quad n = 0, 1, 2, 3 \dots \quad (24)$$

3. Quasiparticle Model and Debye Mass

In the quasiparticle description, the system of the interacting particles is supposed to be noninteracting or in other words weakly interacting by means of the effective fugacity [53] or with the effective mass [54, 55]. Nambu-Jona-Laisino (NJL) and Ploylov Nambu-Jona-Laisino (PNJL) quasiparticle models [56], self-consistent quasiparticle model [57, 58], etc., include the effective masses. Here, we considered the effective fugacity quasiparticle model (EQPM), in the presence of eB , which interprets the QCD EoS as noninteracting quasipartons with effective fugacity parameter z_g for gluons and z_q for quarks encoding all the interacting effects taking place in the medium. The distribution function for the quasiguons and the quasiquarks/quasi-anti-quarks [59] is given in the presence of magnetic field as below:

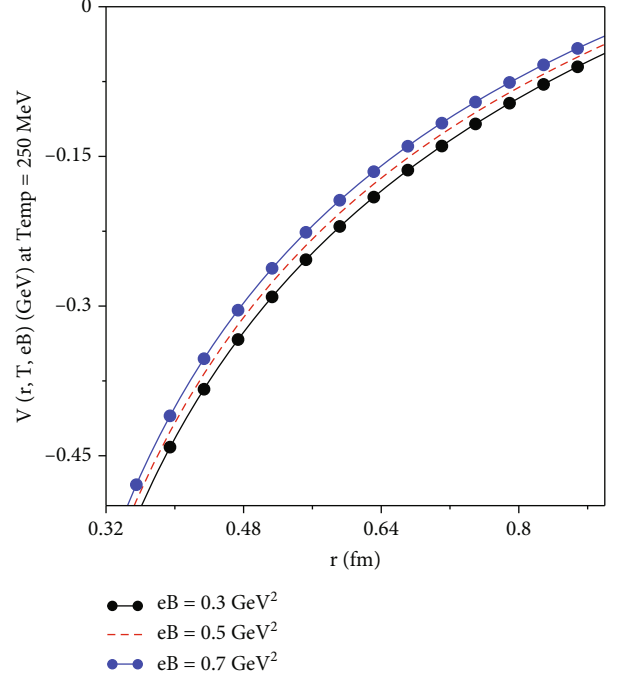


FIGURE 1: The variation of $V(r, T, eB)$ with distance (r) at different values of magnetic field and fixed value of $T = 250$ MeV.

$$f_{g/q} = \frac{f_{g/q} e^{-\beta E_p}}{1 \mp f_{g/q} e^{-\beta E_p}}. \quad (25)$$

To measure the effect of electric potential applied on the QGP, Debye mass played a major role and is gauge invariant and nonperturbative in nature. In this work, we have considered the EQPM which is extended in the presence of magnetic field and interprets the QCD EoS as noninteracting quasipartons with z_q and z_g as the fugacity parameter. So, the distribution function for quark/antiquark is given below:

$$f_q = \frac{z_q e^{-\beta \sqrt{p_z^2 + m^2 + 2l|q_r eB|}}}{1 + z_q e^{-\beta \sqrt{p_z^2 + m^2 + 2l|q_r eB|}}}, \quad (26)$$

where l is the Landau quantum number and eB is the magnetic field. The effect of the magnetic field $B = B\hat{z}$ is taken along the z -axis. Since the plasma contains both the charged and the quasineutral particles, hence it shows collective behavior. Debye mass is an important quantity to describe the screening of the color forces in the hot QCD medium. Debye screening mass can be defined as the ability of the plasma to shield out the electric potential applied to it. In the studies [60–63], detailed definition of the Debye mass can be seen. To determine the Debye mass in terms of the eB , we start from the gluon self-energy as below:

$$m_D^2 = \Pi_{00}(\omega = p, |\vec{p}| \rightarrow 0). \quad (27)$$

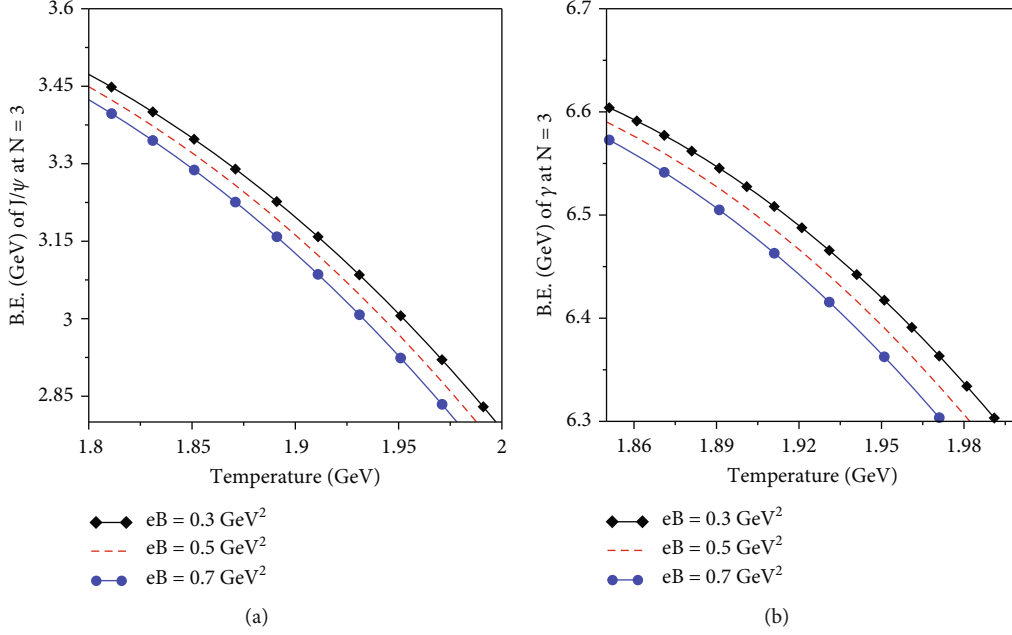


FIGURE 2: Dependence of (a) J/ψ and (b) Y binding energies with temperature for different values of magnetic field at fixed value of $N = 3$.

According to [52], gluon self-energy was modified as follows:

$$\Pi_{00}(\omega = p, |\vec{p}| \rightarrow 0) = \frac{g^2 |eB|}{2\pi^2 T} \int_0^\infty dp_z f_q^0 (1 - f_q^0). \quad (28)$$

Thus, Debye mass for quarks using the distribution function defined by Eq. (26) is given below:

$$m_D^2 = \frac{4\alpha}{\pi T} |eB| \int_0^\infty dp_z f_q^0 (1 - f_q^0). \quad (29)$$

Since, the magnetic field has no effect on the gluon and gluonic contribution to the Debye mass, it will remain intact/unchanged. The other approach to obtain the Debye mass is the kinetic theory approach. Both these approaches provide similar results for the Debye mass in the presence of eB . So, the Debye mass for $N_f = 3$ and $N_c = 3$ will be

$$m_D^2 = 4\alpha \left(\frac{6T^2}{\pi} \text{PolyLog}[2, z_g] + \frac{3eB}{\pi} \frac{z_q}{1+z_q} \right). \quad (30)$$

The Debye mass for the ideal EoS [$z_{q,g} = 1$] representing noninteracting quarks and gluons becomes

$$m_D^2 = 4\pi\alpha \left(T^2 + \frac{3eB}{2\pi^2} \right). \quad (31)$$

4. Binding Energy (B.E.) of Quarkonium State in N -Dimensional Space

The binding energy of quarkonium state such as bottomonium and charmonium has been studied in this section.

By using AEIM, the approximate energy eigenvalues in N -dimensional space becomes

$$\text{B.E.} = E_{nl}^n = \sqrt{\frac{a}{2\mu_{Q\bar{Q}}}} (N + 2l + 2n) + C - \frac{b^2}{4(\sqrt{a})^2}. \quad (32)$$

In this equation, ($n = 0, 1, 2, 3, \dots$) correspond to the state of quarkonia.

5. Mass Spectra of Quarkonium State in N -Dimensional Space

The mass spectra of heavy quarkonia can be calculated by using the relation given below:

$$M = 2m_Q + \text{B.E.} \quad (33)$$

Here, mass spectra are equal to the sum of the energy eigenvalues and twice of the quark-anti-quark mass. Substituting the values of E_{nl}^n in the Eq. (33), we get

$$M = 2m_Q + \sqrt{\frac{a}{2\mu_{Q\bar{Q}}}} (N + 2l + 2n) + C - \frac{b^2}{4(\sqrt{a})^2}, \quad (34)$$

where m_Q is the mass of quarkonium state, l is the angular momentum quantum number, and $\mu_{Q\bar{Q}}$ is the reduced mass.

6. QCD EoS in the Presence of Magnetic Field

The EoS for the quark matter is an important finding in relativistic nucleus-nucleus collisions, and the thermodynamical properties of matter are sensitive to EoS. The

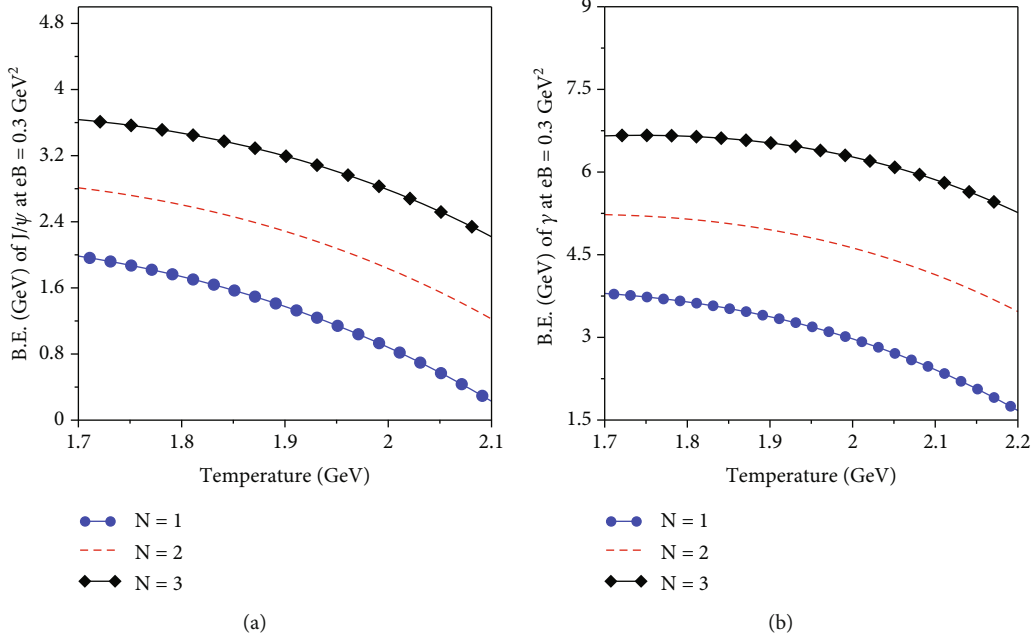


FIGURE 3: Dependence of (a) J/ψ and (b) Y binding energies with temperature for different values of dimensionality number at fixed value of $eB = 0.3 \text{ GeV}^2$.

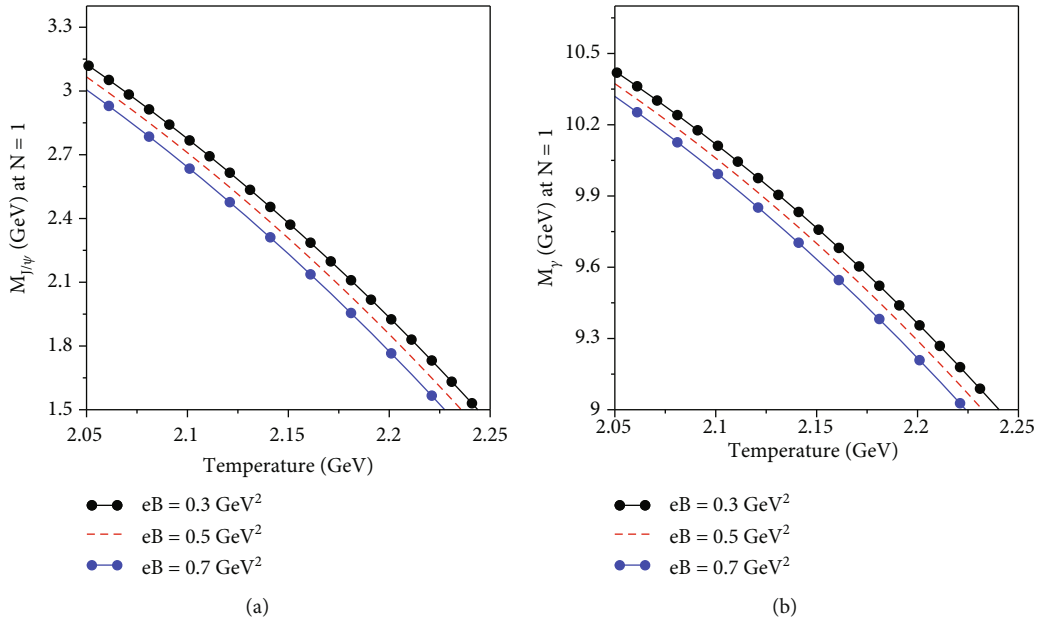


FIGURE 4: Dependence of (a) J/ψ and (b) Y mass spectra with temperature for different values of magnetic field at fixed value of $N = 1$.

EoS which is defined as a function of plasma parameter (Γ) [40] is

$$\varepsilon_{\text{QED}} = \left[\frac{3}{2} + \mu_{\text{ex}}(\Gamma) \right] nT. \quad (35)$$

The ratio of average potential energy to average kinetic energy is known as plasma parameter. Now, let us assume that $\Gamma \ll 1$ and is given by

$$\Gamma \equiv \frac{\langle PE \rangle}{\langle KE \rangle} = \frac{\text{Re} [V(r, T)]}{T}. \quad (36)$$

But after inclusion of relativistic and quantum effects, the EoS which has been already obtained in the Γ can be written as follows:

$$\varepsilon = (3 + \mu_{\text{ex}}(\Gamma))nT. \quad (37)$$

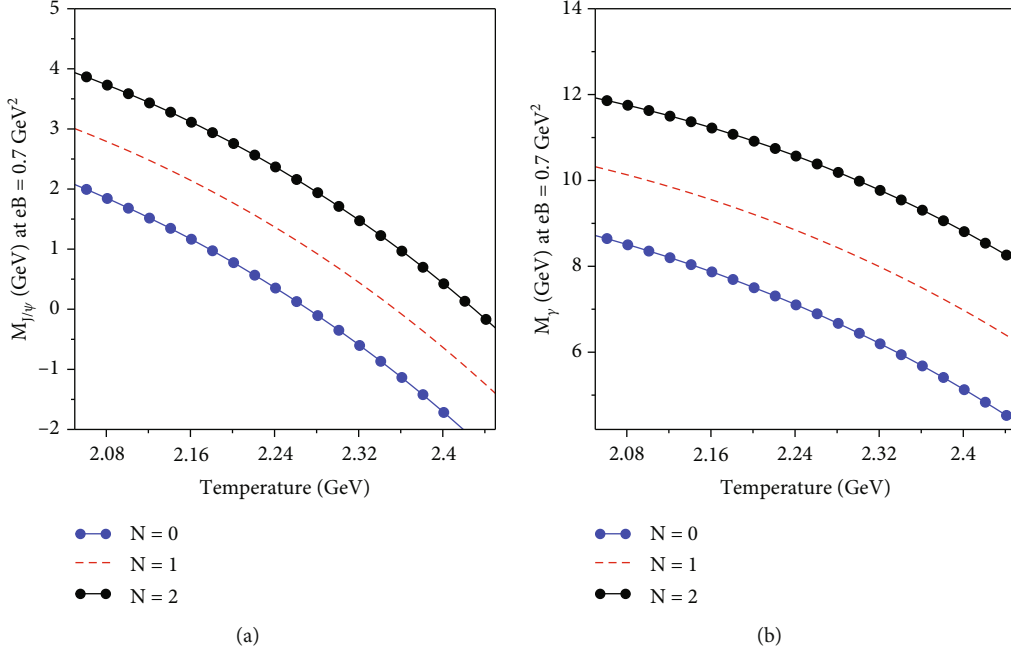


FIGURE 5: Dependence of (a) J/ψ and (b) Y mass spectra with temperature for different values of dimensionality number at fixed value of $eB = 0.7 \text{ GeV}^2$.

TABLE 1: Comparison of the mass spectra for J/ψ and Y obtained in the present work at $N = 1$ with the theoretical and experimental data.

State \downarrow	$eB = 0.3 \text{ GeV}^2$	$eB = 0.5 \text{ GeV}^2$	$eB = 0.7 \text{ GeV}^2$	Solanki et al. [50]	Exp. mass [51]
J/ψ	3.1191	3.0590	3.0161	3.060	3.096
Y	10.4314	10.3824	10.3211	9.200	9.460

The scaled energy density is written as in terms of ideal contribution [50, 52] given below as follows:

$$e(\Gamma) \equiv \frac{\varepsilon}{\varepsilon_{\text{SB}}} = 1 + \frac{1}{3} \mu_{\text{ex}}(\Gamma), \quad (38)$$

where ε_{SB} is

$$\varepsilon_{\text{SB}} \equiv \left(\frac{16 + 21N_f}{2} \right) \frac{\pi^2 T^4}{30}. \quad (39)$$

Here, N_f is the number of flavor of quarks and gluons, and we also consider two-loop level QCD running coupling constant (α) in $\bar{M}\bar{S}$ scheme [50, 52],

$$g^2(T) \approx 2b_0 \ln \frac{\bar{\mu}}{\Lambda_{\bar{M}\bar{S}}} \left(1 + \frac{b_1}{2b_0^2} \frac{\ln(2 \ln(\bar{\mu}/\Lambda_{\bar{M}\bar{S}}))}{\ln(\bar{\mu}/\Lambda_{\bar{M}\bar{S}})} \right)^{-1}, \quad (40)$$

where $b_0 = (33 - 2N_f)/48\pi^2$ and $b_1 = (153 - 19N_f)/384\pi^4$. In $\bar{M}\bar{S}$ scheme, $\Lambda_{\bar{M}\bar{S}}$ and $\bar{\mu}$ are the renormalization scale and the scale parameter, respectively. The dependency of $\Lambda_{\bar{M}\bar{S}}$ is

$$\bar{\mu} \exp(\gamma_E + c) = \Lambda_{\bar{M}\bar{S}}(T), \quad (41)$$

$$\Lambda_{\bar{M}\bar{S}}(T) \exp(\gamma_E + c) = 4\pi\Lambda_T.$$

where $\gamma_E = 0.5772156$ and $c = (N_c - 4N_f \ln 4)/(22N_c - N_f)$ [50, 52]. After using the above relation, first we calculated the energy density ε_T from Eq. (38) and used the thermodynamical relation:

$$\varepsilon = T \frac{dp}{dT} - P. \quad (42)$$

We calculated the pressure [64] as follows:

$$\frac{P}{T^4} = \frac{\left((P_0/T_0) + 3a_f \int_{T_0}^T d\tau \tau^2 \varepsilon(\Gamma(\tau)) \right)}{T^3}, \quad (43)$$

where P_0 is the pressure at some reference temperature T_0 . Now, the speed of sound is calculated by using the relation as follows:

$$c_s^2 = \left(\frac{dP}{d\varepsilon} \right). \quad (44)$$

In this work, we use magnetic field-dependent Debye

TABLE 2: Dissociation of lower bound for $eB=0.3 \text{ GeV}^2$; temperatures are in the unit of T_c by using thermal energy effect criteria.

State \Downarrow	$N = 3$	$N = 4$	$N = 5$
J/ψ	1.3921	1.5109	1.7709
Y	2.0509	2.2509	2.4110

TABLE 3: Dissociation of lower bound for $N = 5$; temperatures are in the unit of T_c by using thermal energy effect criteria.

State \Downarrow	$eB = 0.3 \text{ GeV}^2$	$eB = 0.5 \text{ GeV}^2$	$eB = 0.7 \text{ GeV}^2$
J/ψ	1.7709	1.7591	1.7465
Y	2.4110	2.4009	2.3899

TABLE 4: Dissociation of upper bound for $eB = 0.3 \text{ GeV}^2$; temperatures are in the unit of T_c by using thermal energy effect criteria.

State \Downarrow	$N = 3$	$N = 4$	$N = 5$
J/ψ	2.2109	2.3309	2.4310
Y	2.4710	2.5909	2.7010

TABLE 5: Dissociation of upper bound for $N = 5$; temperatures are in the unit of T_c by using thermal energy effect criteria.

State \Downarrow	$eB = 0.3 \text{ GeV}^2$	$eB = 0.5 \text{ GeV}^2$	$eB = 0.7 \text{ GeV}^2$
J/ψ	2.4310	2.4209	2.4107
Y	2.7010	2.6909	2.6799

mass to address the thermodynamics of the QGP matter in the presence of magnetic field. This is because of the fact that all the thermodynamical properties of the quarkonia are potential dependent which in turn depends on the magnetic field.

7. Dissociation Energy (D.E.) of Quarkonium State in N -Dimensional Space

The most precious quantity to notice the vanishing of bound state is the dissociation energy. The D.E. of heavy quarkonia can be calculated by using the relation given below:

$$\text{D.E.} = E_{\text{dissociation}}^{N,l} \equiv 2m_Q + \frac{\sigma}{m_D} - \text{B.E.} \quad (45)$$

After introducing the value of binding energy in the above expression, we get the final expression of D.E. in N -dimensional space as follows:

$$\text{D.E.} = E_{\text{dissociation}}^{N,l} \equiv 2m_Q + \frac{\sigma}{m_D} - \left[\sqrt{\frac{a}{2\mu_{Q\bar{Q}}}}(N+2l+2n) + C - \frac{b^2}{4(\sqrt{a})^2} \right]. \quad (46)$$

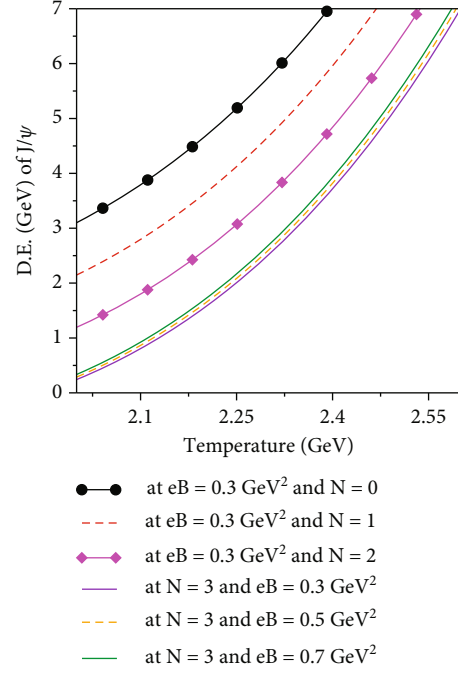


FIGURE 6: The variation of dissociation energy (D.E.) of J/ψ with temperature at different values of magnetic field (eB) and dimensionality number (N).

8. Results and Discussion

In this analysis, we have taken fixed value of critical temperature ($T_c = 197 \text{ MeV}$) throughout the manuscript and various quantities such as binding energy (B.E.) and dissociation temperature, and the mass spectra of the quarkonia have been studied with finite values of magnetic field. The variation of the potential with distance (in fm) at fixed value of temperature ($T = 250 \text{ MeV}$) for different values of magnetic field ($eB = 0.3, 0.5, \text{ and } 0.7 \text{ GeV}^2$) is shown in Figure 1. We clearly noticed that in Figure 1, if we increase the values of magnetic field, then the variation of potential also increases.

Figures 2 and 3 shows the variation of binding energy of J/ψ and Y with temperature. From Figure 1, we can deduce that the values of the binding energy of J/ψ (a) and Y (b) decrease with temperature for different values of the magnetic field ($eB = 0.3, 0.5, \text{ and } 0.7 \text{ GeV}^2$) at fixed value of dimensionality number ($N = 3$). The effect of dimensionality number on the binding energy for the quarkonium state J/ψ (a) and Y (b) with temperature has been shown in Figure 1. If the value of dimensionality number increases, the binding energy of quarkonium states becomes higher at the fixed value of magnetic field ($eB = 0.3 \text{ GeV}^2$).

Figure 4 shows the variation of mass spectra of heavy quarkonia with temperature for 1S state of charmonium J/ψ (a) and 1S state of bottomonium Y (b) for different values of magnetic field ($eB = 0.3, 0.5, \text{ and } 0.7 \text{ GeV}^2$) at fixed value of dimensionality number ($N = 1$). We observed that if we increase the value of magnetic field (at fixed value of mass of ground state of quarkonium, i.e., $m_{J/\psi} = 1.5 \text{ GeV}$ and $m_Y = 4.5 \text{ GeV}$), the variation of mass spectra decreases. Figure 5 also

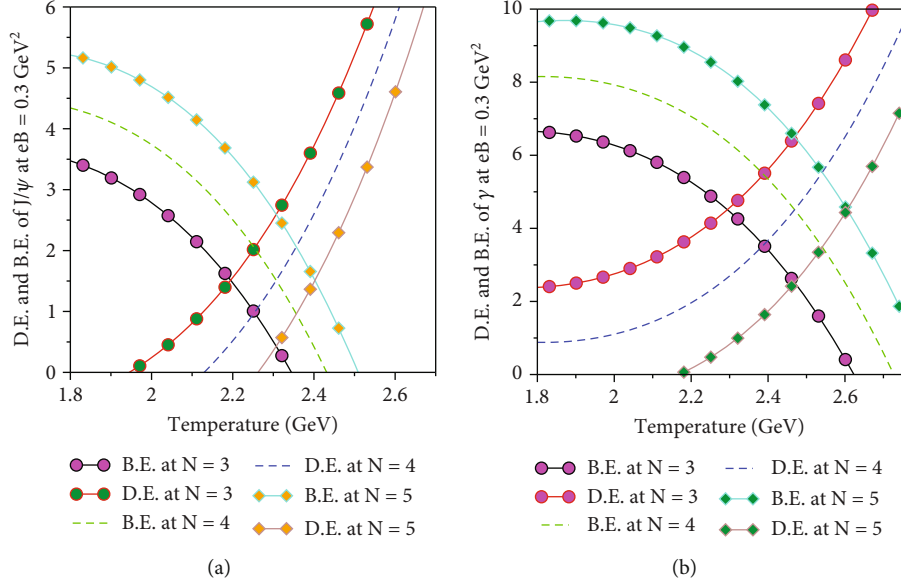


FIGURE 7: The variation of dissociation energy (D.E.) and binding energy (B.E.) of (a) J/ψ and (b) Y with temperature at different values of dimensionality number (N) and fixed value of magnetic field (eB).

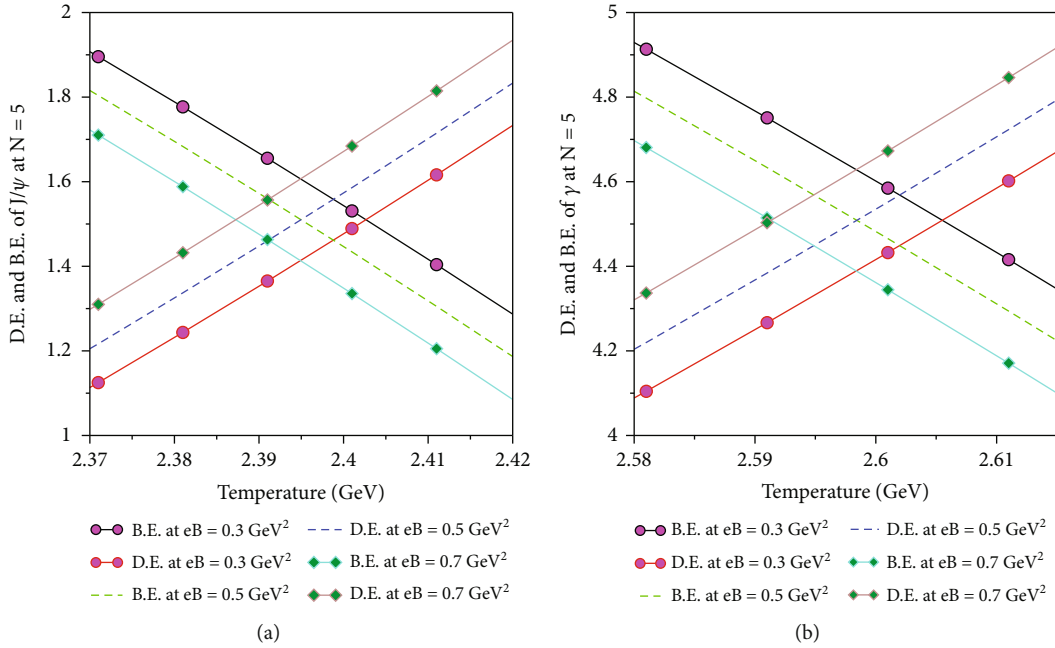


FIGURE 8: The variation of dissociation energy (D.E.) and binding energy (B.E.) of (a) J/ψ and (b) Y with temperature at different values of magnetic field (eB) and fixed value of dimensionality number (N).

TABLE 6: Dissociation temperature for $eB = 0.3 \text{ GeV}^2$; temperatures are in the unit of T_c by using dissociation energy criteria.

State \Downarrow	$N = 3$	$N = 4$	$N = 5$
J/ψ	2.1959	2.3090	2.4055
Y	2.2965	2.4711	2.6079

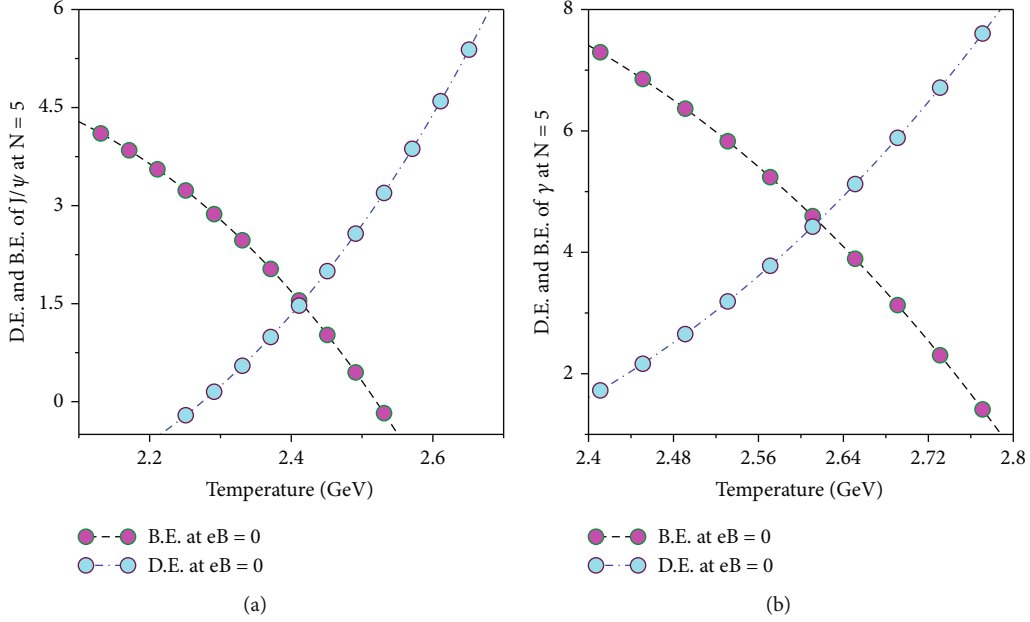
shows the variation of mass spectra of heavy quarkonia with temperature for 1S state of charmonium J/ψ (a) and 1S state of bottomonium Y (b) for different values of dimensionality

number ($N = 0, 1, \text{ and } 2$) at fixed value of magnetic field ($eB = 0.7 \text{ GeV}^2$). We observed that if we increase the values of dimensionality number, the variation of mass spectra also increases. We also compared the value of mass spectra for J/ψ and Y obtained in the present work at different values of magnetic field with the other calculated theoretical and experimental values of mass spectra as shown in Table 1.

The dissociation temperature for real binding energies can be obtained by using thermal energy. According to references [27, 39], it is not necessary to have zero binding energy for dissolution of the quarkonium states. When binding

TABLE 7: Dissociation temperature for $N = 5$; temperatures are in the unit of T_c by using dissociation energy effect criteria.

State \Downarrow	eB = 0	eB = 0.3 GeV ²	eB = 0.5 GeV ²	eB = 0.7 GeV ²
J/ψ	2.4185	2.4055	2.3949	2.3874
Y	2.6162	2.6079	2.5984	2.5913

FIGURE 9: The variation of dissociation energy (D.E.) and binding energy (B.E.) of (a) J/ψ and (b) Y with temperature at $eB = 0$ and fixed value of dimensionality number (N).

energy ($E_{\text{bin}} \leq T$) of quarkonium state is weakly bonded, it dissociates by means of thermal fluctuations. The quarkonium state is also said to be dissociated; when $2B.E. \leq \Gamma(T)$, $\Gamma(T)$ is thermal width of respective quarkonium states. Hence, there are two ways to calculate dissociation point of quarkonia. The lower bound of dissociation using mean thermal energy can be written as follows:

$$\sqrt{\frac{a}{2\mu_{Q\bar{Q}}}}(N + 2l + 2n) + C - \frac{b^2}{4(\sqrt{a})^2} = 3(T_D), \quad (47)$$

and for upper bound, the expression is as follows:

$$\sqrt{\frac{a}{2\mu_{Q\bar{Q}}}}(N + 2l + 2n) + C - \frac{b^2}{4(\sqrt{a})^2} = (T_D), \quad (48)$$

where $\mu_{Q\bar{Q}} = m_c/2$ and $m_b/2$. The dissociation temperatures for the J/ψ and Y have been given in Tables 2–5. Lower bound of dissociation temperature has been shown in Table 2 (at different values of N) and Table 3 (at different values of magnetic field), whereas Table 4 (at different values of N) and Table 5 (at different values of magnetic field) show the different values of dissociation temperatures for upper bound. In general, the dissociation temperature decreases

with the magnetic field and increases with dimensionality number.

The variation of dissociation energy (D.E.) of J/ψ has been shown in Figure 6 with the temperature for different values of magnetic field and dimensionality number. It has been deduced that the D.E. of the quarkonium states with the magnetic field increases, but with the dimensionality number, it decreases. In this manuscript, we have applied one more way to calculate the dissociation temperature with the help of dissociation energy (D.E.) and binding energy. The variation of B.E. and D.E. of the J/ψ in Figures 7(a) and 8(a) and Y in Figures 7(b) and 8(b) with temperature for different values of dimensionality number (Figure 7) and for different values of magnetic field (Figures 8) has been shown, respectively. From Figures 7 and 8, we have examined the dissociation temperature (by intersection point of the D.E. and B.E. of the quarkonia) of the J/ψ and Y for different values of eB and N , and the values of dissociation temperature are given in Tables 6 and 7, respectively. Figure 9 shows the variation of dissociation energy (D.E.) and binding energy (B.E.) of J/ψ (a) and Y (b) with temperature at fixed value of $eB = 0$ and $N = 5$. From Figure 9, we have examined the values of dissociation temperature at zero magnetic field using dissociation energy criteria, and the values has been shown in Table 7 for showing the difference between with or without eB .

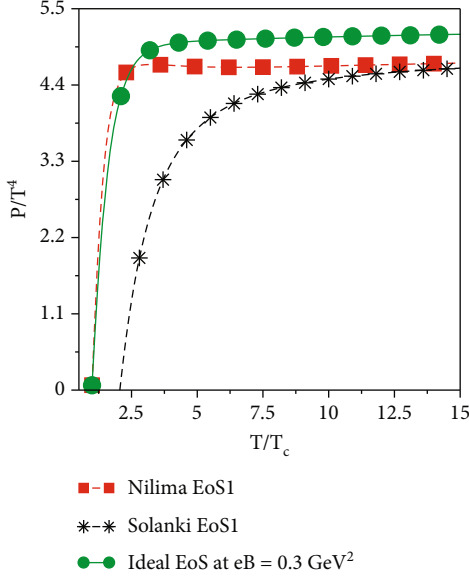


FIGURE 10: Variation of P/T^4 as a function of T/T_c for our ideal EoS at $eB = 0.3 \text{ GeV}^2$ and also compared with the published results of Nilima EoS1 [52] and Solanki EoS1 [50].

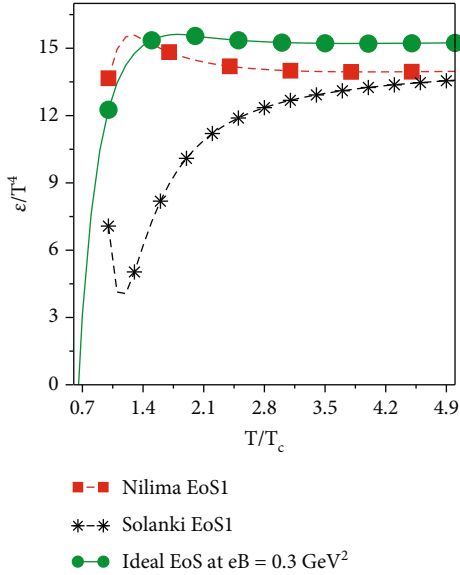


FIGURE 11: Variation of ϵ/T^4 as a function of T/T_c for our ideal EoS at $eB = 0.3 \text{ GeV}^2$ and also compared with the published results of Nilima EoS1 [52] and Solanki EoS1 [50].

The thermodynamical properties of quark matter play a significant role in the study of QGP and also provide useful information about the strange quark matter. In Figures 10–12, we have plotted the variation of pressure (P/T^4), energy density ϵ , and speed of sound (C_s^2) with temperature (T/T_c) at $eB = 0.3 \text{ GeV}^2$ for ideal EoS with 3 flavor QGP. The obtained results are also compared with the results of Nilima EoS1 [52] and Solanki EoS1 [50].

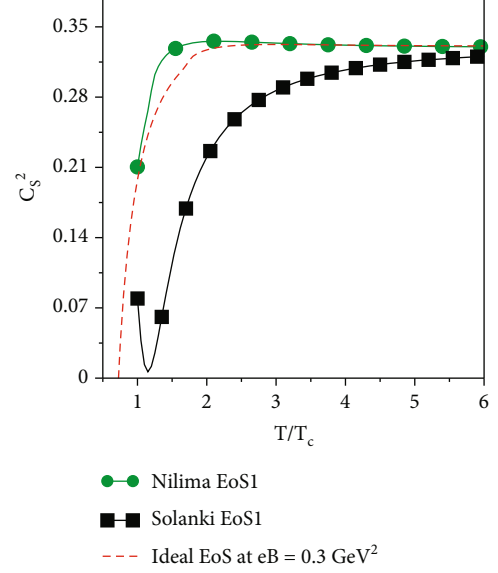


FIGURE 12: Variation of C_s^2 as a function of T/T_c for our ideal EoS at $eB = 0.3 \text{ GeV}^2$ and also compared with the published results of Nilima EoS1 [52] and Solanki EoS1 [50].

9. Conclusion

We have considered the medium-modified form of Cornell potential at finite values of magnetic field and dimensionality number. To reach end, we considered magnetic field-dependent quasiparticle Debye mass for the study of dissociation pattern of quarkonia. Real part of medium-modified form of Cornell potential has been used for solving Schrodinger equation to obtain binding energy of quarkonia in N -dimensional space. We observed that binding energy and mass spectra decrease with increasing the values of eB . However, binding energy and mass spectra tend to get higher with increasing value of N . The variation of dissociation energy with the temperature for different values of eB and N has been shown in Figure 6. It has been seen that the dissociation energy of the quarkonium states with the magnetic field increases, but with the dimensionality number, it decreases.

We applied another way to calculate the dissociation temperature with the help of dissociation energy and binding energy. The variation of B.E. and D.E. of the states of quarkonia with temperature for different values of dimensionality number and for different values of magnetic field has been shown, respectively. From these, we have examined the dissociation temperature at the intersection point of the D.E. and B.E. of the quarkonia for different values of eB and N .

In conclusion, the dissociation temperature of heavy quarkonia decreases with magnetic field and increases with dimensionality number. We have also extended this work, after calculating the thermodynamical properties of QGP (i.e., pressure, energy density, and speed of sound) using the parameters eB and N . In the future, we may extend this work to calculate the nucleus-nucleus suppression with the latest determined value of $\sqrt{s_{NN}}$. Also, we can study about the survival probability or nuclear modification factor of

different quarkonium states w.r.t eB , dimensionality number, transverse momentum, centrality, and rapidity which is the key point to quantify various properties of the medium produced during heavy-ion collisions (HICs) at LHC and RHIC.

Data Availability

Data will be made available on request.

Conflicts of Interest

The authors declare that they have no conflicts of interest.

Acknowledgments

One of the authors, VKA, acknowledges the Science and Engineering Research Board (SERB) Project No. EEQ/2018/000181, New Delhi, for the research support in basic sciences.

References

- [1] S. M. Kuchin and N. V. Maksimenko, "Theoretical estimations of the spin-averaged mass spectra of heavy quarkonia and Bc mesons," *Universal Journal of Physics and Application*, vol. 7, no. 3, pp. 295–298, 2013.
- [2] R. Kumar and F. Chand, "Asymptotic study to the N-dimensional radial Schrödinger equation for the quark-antiquark system," *Communications in Theoretical Physics*, vol. 59, no. 5, pp. 528–532, 2013.
- [3] T. Das, "Treatment of N-dimensional Schroedinger equation for anharmonic potential via Laplace transform," *Electronic Journal of Theoretical Physics*, vol. 13, p. 207, 2016.
- [4] A. Al-Oun, A. Al-Jamel, and H. Widyan, "Various properties of heavy quarkonia from flavor-independent Coulomb plus quadratic potential," *Jordan Journal of Physics*, vol. 4, p. 94, 2015.
- [5] A. N. Ikot, O. A. Awoga, and A. D. Antia, "Bound state solutions of d-dimensional Schrödinger equation with Eckart potential plus modified deformed Hylleraas potential," *Chinese Physics*, vol. 22, no. 2, article 020304, 2013.
- [6] S. M. Al-Jaber, "A confined N-dimensional harmonic oscillator," *International Journal of Theoretical Physics*, vol. 47, no. 7, pp. 1853–1864, 2008.
- [7] S. M. Al-Jaber, "Solution of the radial N-dimensional Schrödinger equation using homotopy perturbation method," *Romanian Journal of Physics*, vol. 58, pp. 247–259, 2013.
- [8] M. Abu-shady, "Multidimensional Schrödinger equation and spectral properties of heavy-quarkonium mesons at finite temperature," *Advances in Mathematical Physics*, vol. 2016, Article ID 4935940, 7 pages, 2016.
- [9] G. R. Khan, "Exact solution of N-dimensional radial Schrödinger equation for the fourth-order inverse-power potential," *The European Physical Journal D*, vol. 53, no. 2, pp. 123–125, 2009.
- [10] S. Ikhdair and R. Sever, "Polynomial solutions of the Mie-type potential in the D-dimensional Schrödinger equation," *Journal of Molecular Structure: Theochem*, vol. 13, p. 855, 2008.
- [11] S. M. Ikhdair and M. Hamzavi, "Spectral properties of quantum dots influenced by a confining potential model," *Physica B*, vol. 407, no. 24, pp. 4797–4803, 2012.
- [12] G. Chen, "Exact solutions of the N-dimensional radial schrödinger equation with the Coulomb potential via the Laplace transform," *Zeitschrift für Naturforschung A*, vol. 59, no. 11, pp. 875–876, 2004.
- [13] H. Hassanabadi, S. Zarrinkamar, and A. A. Rajabi, "Exact solutions of D-dimensional Schrödinger equation for an energy-dependent potential by NU method," *Communications in Theoretical Physics*, vol. 55, no. 4, pp. 541–544, 2011.
- [14] H. Hassanabadi, B. H. Yazarloo, S. Zarrinkamar, and M. Solaimani, "Approximate analytical versus numerical solutions of Schrödinger equation under molecular Hua potential," *International Journal of Quantum Chemistry*, vol. 112, no. 23, pp. 3706–3710, 2012.
- [15] G. R. Boroun and H. Abdolmalki, "Variational and exact solutions of the wavefunction at origin (WFO) for heavy quarkonium by using a global potential," *Physica Scripta*, vol. 80, no. 6, article 065003, 2009.
- [16] R. N. Choudhury and M. Mondal, "Eigenvalues of anharmonic oscillators and the perturbed Coulomb problem in N-dimensional space," *Physical Review A*, vol. 52, no. 3, pp. 1850–1856, 1995.
- [17] L. G. Ixaru, H. De Meyer, and G. V. Berghe, "Highly accurate eigenvalues for the distorted Coulomb potential," *Physical Review E*, vol. 61, no. 3, pp. 3151–3159, 2000.
- [18] P. Sandin, M. Ögren, and M. Gulliksson, "Numerical solution of the stationary multicomponent nonlinear Schrödinger equation with a constraint on the angular momentum," *Physical Review E*, vol. 93, no. 3, article 033301, 2016.
- [19] Z. Wang and Q. Chen, "A trigonometrically-fitted one-step method with multi-derivative for the numerical solution to the one-dimensional Schrödinger equation," *Computer Physics Communications*, vol. 179, p. 49, 2005.
- [20] E. Z. Liverts, E. G. Drukarev, R. Krivec, and V. B. Mandelzweig, "Analytic presentation of a solution of the Schrödinger equation," *Few Body Systems*, vol. 44, no. 1-4, pp. 367–370, 2008.
- [21] R. De, R. Dutt, and U. Sukhatme, "Mapping of shape invariant potentials under point canonical transformations," *Journal of Physics A: Mathematical and General*, vol. 25, no. 13, pp. L843–L850, 1992.
- [22] J. J. Sakurai, *Modern Quantum Mechanics*, Addison-Wesley Publishing, New York, 1967.
- [23] D. Agboola, "The Hulthén potential in D-dimensions," *Physica Scripta*, vol. 80, no. 6, article 065304, 2009.
- [24] R. Kumar and F. Chand, "Series solutions to the N-dimensional radial Schrödinger equation for the quark-antiquark interaction potential," *Physica Scripta*, vol. 85, no. 5, article 055008, 2012.
- [25] E. M. Khokha, M. Abu-Shady, and T. A. Abdel-Karim, "Quarkonium masses in the N-dimensional space using the analytical exact iteration method," 2016, <https://arxiv.org/abs/1612.08206>.
- [26] H. Rahimov, H. Nikoofard, S. Zarrinkamar, and H. Hassanabadi, "Any l-state solutions of the Schrödinger equation for the modified Woods–Saxon potential in arbitrary dimensions," *Applied Mathematics and Computation*, vol. 219, no. 9, pp. 4710–4717, 2013.
- [27] D. Kharzeev, L. McLerran, and H. Satz, "Non-perturbative quarkonium dissociation in hadronic matter," *Physics Letters B*, vol. 356, no. 2-3, pp. 349–353, 1995.

- [28] H. Vija and M. H. Thoma, "Braaten-Pisarski method at finite chemical potential," *Physics Letters B*, vol. 342, no. 1-4, pp. 212-218, 1995.
- [29] L. Thakur, N. Haque, U. Kakade, and B. K. Patra, "Dissociation of quarkonium in an anisotropic hot QCD medium," *Physical Review D*, vol. 88, no. 5, article 054022, 2013.
- [30] S. Chao-Yi, J. Q. Zhu, and Z. L. Ma, "Thermal width for heavy quarkonium in the static limit," *Chinese Physics Letters*, vol. 32, no. 12, article 121201, 2015.
- [31] L. Thakur and B. K. Patra, "Quarkonium dissociation in an anisotropic QGP," *Journal of Physics: Conference Series*, vol. 668, article 012085, 2016.
- [32] V. K. Agotiya, V. Chandra, M. Y. Jamal, and I. Nilima, "Dissociation of heavy quarkonium in hot QCD medium in a quasi-particle model," *Physical Review D*, vol. 94, no. 9, article 094006, 2016.
- [33] H. Gervais and S. Jeon, "Photon production from a quark-gluon plasma at finite baryon chemical potential," *Physical Review C*, vol. 86, no. 3, article 034904, 2012.
- [34] A. Monnai, "Dissipative hydrodynamic effects on baryon stopping," *Physical Review C*, vol. 86, no. 1, article 014908, 2012.
- [35] S. S. Singh, "Free energy and direct photon emission at finite chemical potential," *Journal of Physics: Conference Series*, vol. 535, article 012002, 2014.
- [36] V. S. Filinov, V. E. Fortov, M. Bonitz, and Z. Moldabekov, "Fermionic path-integral Monte Carlo results for the uniform electron gas at finite temperature," *Contributions to Plasma Physics*, vol. 91, no. 3, 2015.
- [37] S. M. Sanches, D. A. Fogaca, F. S. Navarra, and H. Marrochio, "Cavitation in a quark gluon plasma with finite chemical potential and several transport coefficients," *Physical Review C*, vol. 92, no. 2, article 025204, 2015.
- [38] W. M. Alberico, A. Beraudo, A. De Pace, and A. Molinari, "Quarkonia in the deconfined phase: effective potentials and lattice correlators," *Physical Review D*, vol. 75, no. 7, article 074009, 2007.
- [39] A. Mocsy and P. Petreczky, "Quarkonia in the quark gluon plasma," *Physical Review Letters*, vol. 99, no. 21, article 211602, 2007.
- [40] V. Agotiya, V. Chandra, and B. K. Patra, "Dissociation of quarkonium in a hot QCD medium: modification of the interquark potential," *Physical Review C*, vol. 80, no. 2, article 025210, 2009.
- [41] S. Solanki, M. Lal, and V. K. Agotiya, "Study of differential scattering cross-section using Yukawa term of medium-modified Cornell potential," *Advances in High Energy Physics*, vol. 2022, Article ID 1456538, 12 pages, 2022.
- [42] S. Solanki, M. Lal, and V. K. Agotiya, "Quarkonium dissociation properties of hot QCD medium at momentum anisotropy in the N-dimensional space using quasi-particle Debye mass with finite baryonic chemical potential," <https://arxiv.org/abs/2105.12346>.
- [43] A. Dumitru, Y. Guo, A. Mocsy, and M. Strickland, "Quarkonium states in an anisotropic QCD plasma," *Physical Review D*, vol. 79, no. 5, article 054019, 2009.
- [44] M. Margotta, K. McCarty, C. McGahan, M. Strickland, and D. Yager-Elorriaga, "Quarkonium states in a complex-valued potential," *Physical Review D*, vol. 83, no. 10, 2011.
- [45] S. Iwasaki, M. Oka, and K. Suzuki, "A review of quarkonia under strong magnetic fields," *The European Physical Journal A*, vol. 57, no. 7, p. 222, 2021.
- [46] I. Nilima, A. Bandyopadhyay, R. Ghosh, and S. Ghosh, "Heavy quark potential and LQCD based quark condensate at finite magnetic field," *European Physical Journal C: Particles and Fields*, vol. 83, no. 1, p. 30, 2023.
- [47] M. Abu-Shady, T. A. Abdel-Karim, and E. M. Khokha, "Binding energies and dissociation temperatures of heavy quarkonia at finite temperature and chemical potential in the N-dimensional space," *Advances in High Energy Physics*, vol. 2018, Article ID 7356843, 12 pages, 2018.
- [48] A. O. Barut, M. Berrondo, and G. Garcia-Calderon, "Narrow resonances as an eigenvalue problem and applications to high energy magnetic resonances: an exactly soluble model," *Journal of Mathematical Physics*, vol. 21, no. 7, pp. 1851-1855, 1980.
- [49] S. Ozelik and M. Simsek, "Exact solutions of the radial Schrödinger equation for inverse-power potentials," *Physics Letters A*, vol. 152, no. 3-4, pp. 145-150, 1991.
- [50] S. Solanki, M. Lal, R. Sharma, and V. K. Agotiya, "Study of quarkonium properties using SUSYQM method with baryonic chemical potential," *International Journal of Modern Physics A*, vol. 37, no. 31n32, article 2250196, 2022.
- [51] M. Tanabashi, K. Hagiwara, K. Hikasa et al., "Review of Particle Physics," *Physical Review D*, vol. 98, no. 3, article 030001, pp. 546-548, 2018.
- [52] I. Nilima and V. K. Agotiya, "Bottomonium suppression in nucleus-nucleus collisions using effective fugacity quasi-particle model," *Advances in High Energy Physics*, vol. 2018, Article ID 8965413, 12 pages, 2018.
- [53] V. Chandra and V. Ravishanker, "Quasi-particle model for lattice QCD: quark-gluon plasma in heavy ion collisions," *European Physical Journal C: Particles and Fields*, vol. 64, no. 1, pp. 63-72, 2009.
- [54] V. Goloviznin and H. Satz, "Extreme states of matter in strong interaction physics: an introduction," *Z Physics C*, vol. 57, p. 671, 1994.
- [55] A. Peshier, B. Kampfer, O. P. Pavlenko, and G. Soff, "Massive quasiparticle model of the SU(3) gluon plasma," *Physics Letters D*, vol. 54, no. 3, pp. 2399-2402, 1996.
- [56] A. Dumitru and R. D. Pisarski, "Degrees of freedom and the deconfining phase transition," *Physics Letters B*, vol. 525, no. 1-2, pp. 95-100, 2002.
- [57] V. M. Bannur, "Self-consistent quasiparticle model for quark-gluon plasma," *Physics Letters C*, vol. 75, no. 4, article 044905, 2006.
- [58] V. M. Bannur, "Comments on quasiparticle models of quark-gluon plasma," *Physics Letters B*, vol. 647, no. 4, pp. 271-274, 2007.
- [59] M. Kurian and V. Chandra, "Bulk viscosity of a hot QCD medium in a strong magnetic field within the relaxation-time approximation," *Physics Letters D*, vol. 97, no. 11, article 116008, 2018.
- [60] A. Rebhan, "Non-Abelian Debye mass at next-to-leading order," *Physics Letters D*, vol. 48, no. 9, pp. R3967-R3970, 1993.
- [61] E. Shuryak, "Theory of hadron plasma," *Journal Article: Theory of Hadron Plasma*, vol. 47, no. 2, p. 212, 1978.

- [62] S. Mrowczynski, "Topics in the transport theory of quark gluon plasma," *Physics of Particles and Nuclei*, vol. 30, no. 4, p. 419, 1999.
- [63] K. Yagi, T. Hatsuda, and Y. Miake, "Quark-gluon plasma: from big bang to little bang," *Cambridge Monographs on Particle Physics, Nuclear Physics and Cosmology*, vol. 23, pp. 1–446, 2005.
- [64] S. Solanki, M. Lal, R. Sharma, and V. K. Agotiya, "Dissociation and thermodynamical properties of heavy quarkonia in an anisotropic strongly coupled hot quark gluon plasma: using a baryonic chemical potential," *Physics Letters C*, vol. 109, no. 2, article 024905, 2024.